strain
An International Journal for Experimental Mechanics

Crack-Tip Stress Field and Fatigue Crack Growth Monitoring Using Infrared Lock-In Thermography in A359/SiCp Composites

D. P. Myriounis*†, E. Z. Kordatos*, S. T. Hasan† and T. E. Matikas*

*Department of Materials Science & Engineering, University of Ioannina, 45110, Ioannina, Greece

†Materials & Engineering Research Institute, Sheffield Hallam University, City Campus, S1 1WB, Sheffield, UK

ABSTRACT: This paper deals with the study of fracture behaviour of silicon carbide particle-reinforced aluminium alloy matrix composites (A359/SiCp) using an innovative non-destructive method based on lock-in thermography. The heat wave, generated by the thermo-mechanical coupling and the intrinsic energy dissipated during mechanical cyclic loading of the sample, was detected by an infrared camera. The coefficient of thermo-elasticity allows for the transformation of the temperature profiles into stresses. A new procedure was developed to determine the crack growth rate using thermographic mapping of the material undergoing fatigue. The thermographic results on the crack growth rate of A359/SiCp composite samples with three different heat treatments were correlated with measurements obtained by the conventional compliance method. The results obtained by the two methods were found to be in agreement, demonstrating that lock-in thermography is a powerful tool for fracture mechanics studies. The paper also investigates the effect of heat treatment processing of metal matrix composites on their fracture properties.

KEY WORDS: *fatigue crack growth, heat treatment, lock-in thermography, Metal Matrix Composites (MMCs), particulate reinforced aluminium alloy*

Introduction

Infrared lock-in thermography is one of several non-destructive testing techniques which can be used for defect detection in materials such as metal matrix composites. Silicon carbide particulate-reinforced aluminium matrix composites exhibit improved physical and mechanical properties as compared to the wrought matrix alloy. The use of SiC particulate-reinforced aluminium alloy composites as a substitute of monolithic aluminium alloys in structural applications, especially in the aerospace and automobile industry, is becoming increasingly attractive [1]. In the aerospace industry, where inspection is of main importance at all fabrication stages, there is a need for fast, reliable inspection techniques. Infrared thermography can fulfil this need because it is a quick, full-field and real-time inspection tool, which can examine a relatively large area of a structure. It is also a non-contact technique; the equipment is fairly portable and hence and can be used reasonably easily in the field [2].

A359/SiCp composites exhibit improved properties including high specific modulus, high creep strength, high fatigue resistance, low thermal expansion, and good thermal stability. The tensile ductility and fracture properties of the composites reported to date, however, have lower values than those of the monolithic alloy material and this behaviour is mainly attributed to the introduction of the brittle reinforcement. The introduction of the reinforcement plays a key role in both mechanical and thermal ageing behaviour of the composite material. Particulate-reinforced composites are not homogeneous materials; hence bulk material properties not only are sensitive to the constituent properties but also strongly depend on the properties of interface. Micro-compositional changes which occur during the thermo-mechanical forming process of these materials can cause substantial changes in mechanical properties, such as ductility, fracture toughness and stress corrosion resistance. Therefore, properties as shown in Table 1 have been improved by heat treatment processing. There are still prospects of improvement in order to minimise the effects of the brittle reinforcement behaviour introduced in the ductile matrix. Thus, the interfacial strengthening mechanisms through precipitation hardening can

doi: 10.1111/j.1475-1305.2009.00665.x

Table 1: Mechanical properties of A359/SiCp composites

Material	Condition	$\sigma_{0.2}$(MPa)	σ_{uts}(MPa)	ϵ (%)	E	$HV_{0.5}$
Rolled A359 /SiC/31p	T1	158	168	1	108	150
	HT1	155	187	2	110	182
	T6	321	336	1.3	116	236

improve the properties of the MMC. Table 1 shows the mechanical material property data for A359/SiCp composite system [3].

The microstructure and mechanical properties of particulate reinforced aluminium composites can be altered by thermo-mechanical treatments as well as by changing the reinforcement volume fraction. The strengthening of a pure metal is carried out by alloying and supersaturating to an extent that on suitable heat treatment the excess alloying additions precipitate out (ageing). Properties in particulate metal matrix composites are primarily dictated by the uniformity of the second-phase dispersion in the matrix. The distribution is controlled by solidification and can be later modified during secondary processing. In particular, due to the addition of magnesium in A359, the mechanical properties of this alloy can be greatly improved by a heat treatment process. There are many different heat treatment sequences and each one can modify the microstructural behaviour as desired [3].

In the case of particle-reinforced metals, numerous studies have focused on understanding the influence of crack growth rate [4–6] and the reinforcing particles on the matrix microstructure and the corresponding effect on the fatigue behaviour of the metal matrix composites (MMCs) [7–11]. When a crack propagates through the A359/SiCp composite there are three possible routes. First, through the matrix where there is a ductile propagation, second through the SiC reinforcement where there is a brittle propagation, and thirdly through the particulate/matrix interface where the propagation can be sustained by its strength. It takes more energy for a crack to propagate through an interface and this is the ideal situation for a material to resist fracture. Stresses arising by the crack propagation are ideally sustained by the interface strength; therefore, the crack requires more energy in order to propagate (Figure 1). Precipitation hardening mechanisms can play an important role in strengthening mechanisms and in tailoring the A359/SiCp interface behaviour [3].

In this paper, the fatigue crack propagation was monitored using infrared thermography and the crack-tip stress field has been mapped using thermoelasticity principles. This research completes previous work in which crack growth rates from

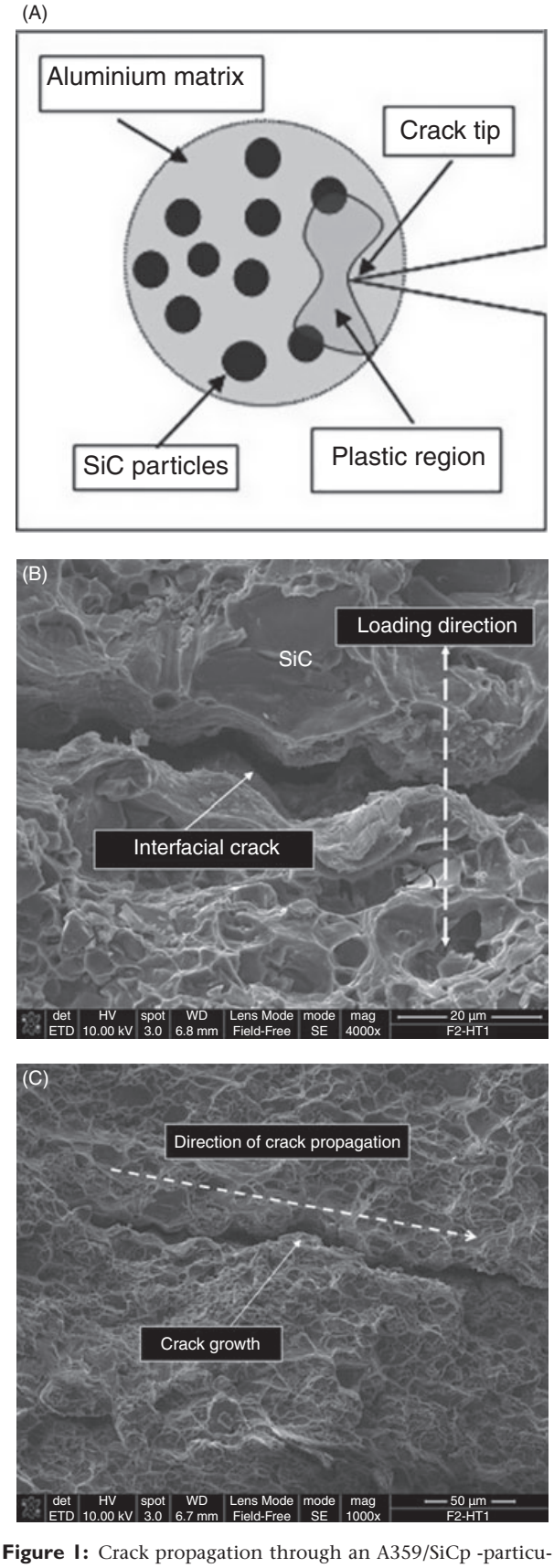

Figure 1: Crack propagation through an A359/SiCp -particulate composite: (A) Schematic of a crack propagation through the particulate-matrix interface, (B) SEM fractography image of an interfacial crack, and (C) SEM fractography image at a lower magnification showing crack growth in an A359/SiCp composite

doi: 10.1111/j.1475-1305.2009.00665.x

thermoelastic data have been considered [12–14]. The technique is based on the fact that when a solid material is rapidly stressed by external or internal loads and adiabatically deformed, the phenomenon is accompanied by simultaneous variation of temperature. When the material is under tensile load, its temperature decreases proportionally to the load, however, when it is under compressive load its temperature increases proportionally to the load. This behaviour is known as the thermoelastic effect.

The thermoelastic effect refers to the thermodynamic relationship between the change of stress in a component under elastic loading and the corresponding change of temperature. It is simply proportional to the change in the sum of the principal stresses, if adiabatic conditions prevail. An experimental setup can be used to map the distribution of the sum of principal stresses in the structure [15]. This setup includes a radiometric camera, which measures the infrared radiation produced on the surface of the material undergoing cyclic loading, and a real-time correlator called 'lock-in module', which measures the slight change of temperature extracting it from the noise that is specified by the thermal resolution of the camera.

The relationship between the thermal stress and strain in an isotropic, elastic element is given by the following equation:

$$\Delta\varepsilon = \frac{(1-2\nu)\cdot\Delta\sigma}{E} + 3\alpha\Delta T \tag{1}$$

where $\Delta\epsilon$ and $\Delta\sigma$ represent the change in the sum of principal strains and stresses, respectively ($\Delta\epsilon$ and $\Delta\sigma$ are invariants). E is Young's modulus, ν is Poisson's ratio, α is the linear thermal expansion coefficient, and ΔT is the change in temperature in degrees Kelvin.

A thermodynamic analysis of reversible, adiabatic behaviour of a stressed, elastic element produces the equation below:

$$\Delta T = \frac{-3T\alpha K\Delta\varepsilon}{\rho C_v} \tag{2}$$

where T is the absolute temperature, K is the bulk modulus, ρ is the density, and C_v is the specific heat at constant volume.

By using the known relationship between C_v and C_p, the specific heat at constant pressure, Equations (1) and (2) may be combined to obtain the following basic equation describing the thermoelastic effect.

$$\Delta T = -\frac{\alpha}{\rho C_p} T\Delta\sigma \tag{3}$$

This relation is only valid if adiabatic conditions prevail. For thermoelastic stress analysis applications, an adiabatic condition is achieved by cyclic loading of the structure, in which case a dynamic equilibrium (i.e. reversibility) is maintained between mechanical and thermal forms of energy. Equation (3) is a general thermodynamic equation quantifying temperature changes produced by changes in the applied stress. The minus sign in the equation means that tension (i.e., $\Delta\sigma$ positive) produces a decrease in temperature, while compression results in an increase in temperature. The change of temperature is proportional to the change in the sum of principal stresses, if adiabatic conditions exist. The thermoelastic coefficient is then given by:

$$K_m = \frac{\alpha}{\rho C_p} \tag{4}$$

Particulate-reinforced composites are not homogeneous materials in the micro-scale. However, for the thermographic measurements the material can be considered as macroscopically homogeneous and isotropic and therefore, Equation (4) is perfectly valid.

The purpose of this research is to develop a new non-destructive methodology based on lock-in thermography for studying the fracture behaviour of A359/SiCp composites by determining the crack growth rate of the specimen undergoing fatigue. The new method is also applied for investigating the influence of heat treatment processing on the fracture properties of the material.

Materials and Experimental Procedures

Heat treatment

The metal matrix composite studied in this work consisted of an aluminium – silicon – magnesium alloy matrix A359, reinforced with silicon carbide particles. Hot rolled A359 aluminium alloy reinforced with 31% SiC particles per weight with an average particle size of 17 ± 1 μm was tested (Figure 2). Table 2 shows the chemical composition of the matrix alloy. Two different heat treatments were applied. T1 condition is the as received condition [16, 17]:

1 In the solution heat treatment T6 the material was heated to a temperature just below the initial melting point of the alloy for 2 h at 530 ± 5 °C. Thus, all the solute atoms were allowed to dissolve to form a single-phase solid solution before being quenched in water. Next, the composites were heated to a

doi: 10.1111/j.1475-1305.2009.00665.x

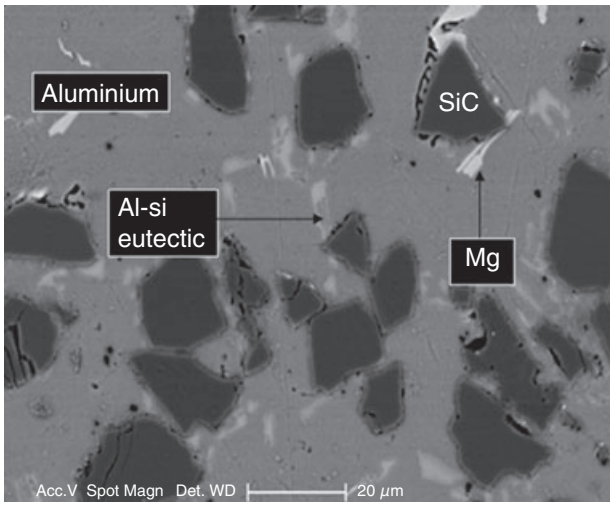

Figure 2: Aluminium alloy/Silicon Carbide particulate Composite

Table 2: Chemical composition of the silicon carbide particulate-reinforced A359 aluminium alloy matrix composite

	Elements (wt %)					
Material	Si	Mg	Mn	Cu	Fe	Zn
A359/SiC_P (31%)	9.5	0.5	0.1	0.2	0.2	0.1

temperature of 155 °C for 5 h and subsequently cooled in air.

2 In the solution heat treatment HT-1 the material was heated to a temperature lower than the T6 condition that is 450 ± 5 °C for 1 h, and then quenched in water. Subsequently, the alloy was heated to an intermediate temperature of 170 °C for 24 h in the age hardened stage and then cooled in air.

Lock–in thermography

Thermography is an advanced NDE technique based on the detection of infrared radiation. Lock-in thermography is an active technique in which the sample is subjected to modulated heating. This technique is based on thermal waves generated inside a specimen and detected remotely by an IR camera. The principle of lock-in thermography is based on the synchronisation of the camera with the source of heating, which can be optical excitation, ultrasound, cyclic loading of the material, etc. In the case that a specimen undergoes cyclic loading, heat waves are generated and the resulting oscillating temperature field in the stationary regime is recorded remotely through thermal infrared emission. The frequency of modulation varies with the nature, size and shape of the defects to be detected. The IR radiation emitted by the specimen during testing depends on the size and shape of the defects to be detected. Using this method, the influence of emissivity and non-uniform heating on the temperature measurement is reduced allowing inspection of large areas of samples with high repeatability and sensitivity. The size of the area for thermographic imaging is 320 × 240 pixels with a pitch of 30 μm × 30 μm. In the experiments the measurement temperature range was between 5–40 °C with a resolution of 20 mK and integration time of 100 ms. The capability of the camera's integration time is 1500 μs.

Lock–in refers to the necessity to monitor the exact time-dependence between the output signal and the reference input signal [18]. This is done using a lock–in amplifier so that both phase and magnitude images become available (Figure 3).

The deformation of solid materials is almost always accompanied by heat release. When the material becomes deformed or it is damaged and fractured, a part of the energy necessary to initiate and propagate the damage is transformed in an irreversible way into heat [19, 20]. The heat wave, generated by the thermo-mechanical coupling and the intrinsic dissipated energy during mechanical loading of the sample was detected by the thermal camera. In this study, the environmental temperature of the sample was kept constant and the raise in temperature on the sample's surface due to fatigue was measured using thermography, allowing the stress field on the sample to be monitored as a function of fatigue cycles.

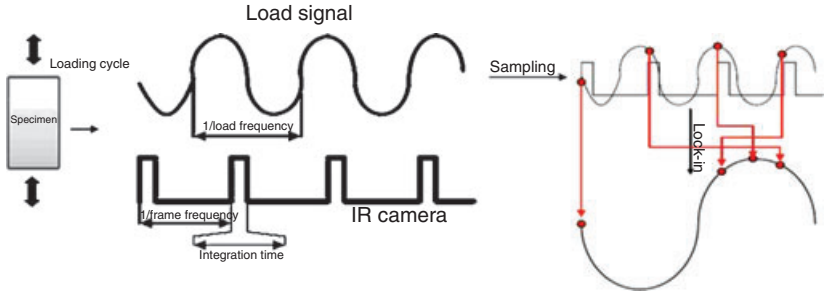

Figure 3: Principle of lock-in thermography

doi: 10.1111/j.1475-1305.2009.00665.x

Fatigue crack growth test

Fatigue crack growth tests were conducted according the ASTM E647 standard, using a 100 kN Instron 8801 servo hydraulic universal testing machine [21]. The test was conducted under load control.

Compact tension (CT) specimens were prepared for fatigue crack growth tests. Throughout the study, all tests were carried out at a frequency of 1 Hz, at a load ratio $R = 0.25$ and load range of 3.7–4.5 kN according to the heat treatment condition of composites. The geometry of the sample is shown in Figure 4.

The technique used for determining the crack growth rate during the test is based on non-contact monitoring the crack propagation by lock-in thermography. For this reason, an infrared camera was placed at a distance close to the specimen. The model of infrared camera is Cedip Jade III MW (Mid wave) InSb. The camera was connected with the lock-in amplifier and the amplifier with the main servo hydraulic controller. Therefore, synchronisation of the frequency through the lock-in amplifier (Cedip R-9902) and the testing machine could be achieved and lock-in images and data capture during the fatigue testing were enabled (Figure 5). The fatigue specimen was not undergone any special polishing preparation for obtaining thermographic data. Flat black mat paint of emissivity $\epsilon = 0.97$ was only applied on the specimen in order to have an emissivity close to that of black body ($\epsilon = 1$). In this way, optimum conditions for thermographic imaging were used.

In order to determine crack growth rate using thermographic mapping of the material undergoing fatigue a simple procedure was used:

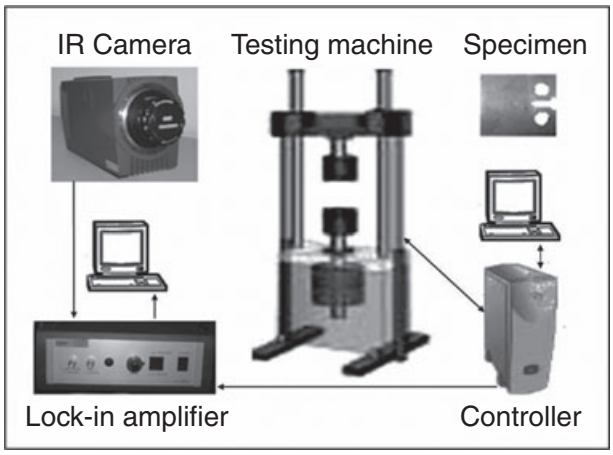

Figure 5: Experimental setup for fatigue crack growth monitoring using lock-in thermography

1 The distribution of temperature and stresses at the surface of the specimen was monitored during the test. To this end, thermal images were obtained as a function of time and saved in the form of a movie.

2 The stresses were evaluated in a post-processing mode, along a series of equally spaced reference lines of the same length, set in front of the crack-starting notch. The idea was that the stress monitored at the location of a line versus time (or fatigue cycles) would exhibit an increase while the crack approaches the line, then attain a maximum when the crack tip was on the line. Due to the fact that the crack growth path could not be predicted and was not expected to follow a straight line in front of the notch, the stresses were monitored along a series of lines of a certain length, instead of a series of equally spaced

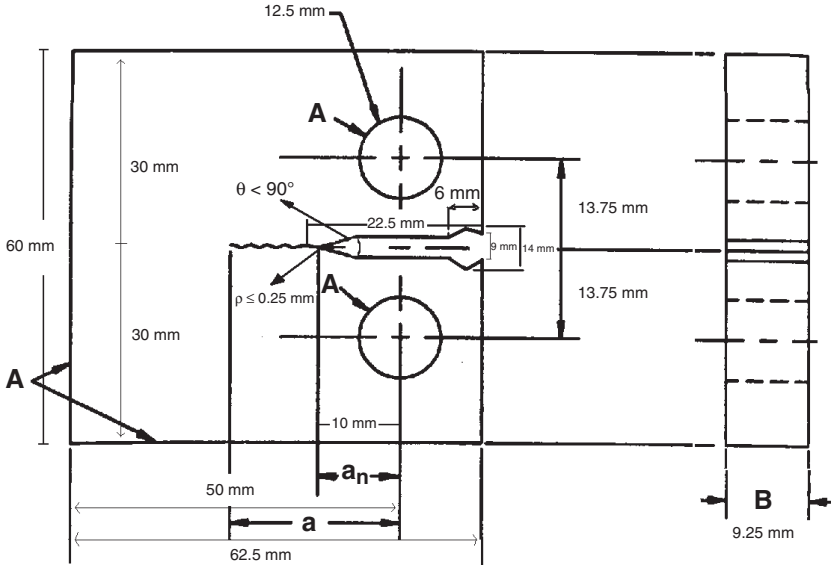

Figure 4: CT specimen geometry

points in front of the notch. The exact path of the crack could be easily determined by looking at the stress maxima along each of these reference lines.

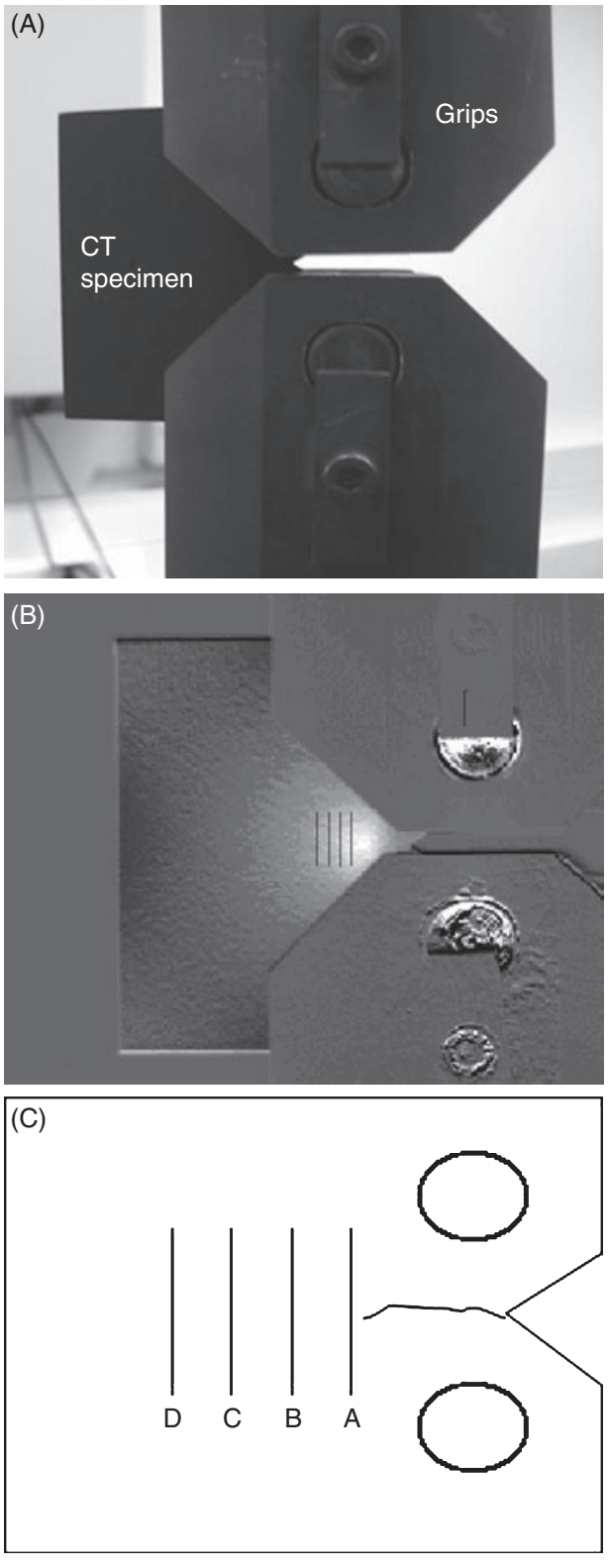

Figure 6: (A) Optical image of the CT specimen on the grips. (B) Thermal image of the CT specimen with the four lines set. (C) Schematic of CT specimen showing 4 lines vertical to the crack propagation direction. These lines were set at a distance from 17 to 20 mm from the notch with equal spacing at a distance of 1 mm

Four lines of the same length, equally spaced at a distance of 1 mm, were set on the thermal images of the CT specimen, as shown in Figure 6. The length of each line is 10 mm long. Line A was set at a distance of 17 mm from the specimen's notch, line B at 18 mm, line C at 19 mm, and line D at 20 mm.

Results and Discussion

Using the procedure described in the previous section, the local stress versus time was measured along each of the four reference lines placed in front of the notch (Figure 7A). The maximum value of stress versus the number of fatigue cycles was then plotted for the four different lines (Figure 7A). As expected, Figure 7A shows that the local stress, monitored at the location of each line, increases while the crack is approaching that line, then attains a maximum when the crack tip is crossing the line. Finally, after the crack has crossed the line, the local stress measured at the location of the line decreases. This is also expected, since the stress values shown in Figure 7A are maximum stresses from all the locations along the particular line. At the exact position on a line where the crack has crossed, the local stress is off coarse null. Figure 7B shows an example of the maximum stress monitored along a reference line, in this case Line D, for a specific time, corresponding to a certain number of fatigue cycles of 13 000 cycles. The total maximum values measured along a line for different number of cycles are then plotted versus the number of cycles, as shown in Figure 7A for four different reference lines.

The actual thermographic images shown in Figure 8 correspond to the 4 different reference lines showing the crack propagation length and the stress field for each of these lines. It can be clearly seen that as crack propagates the stress field changes accordingly (clearly shown with white areas formed on the specimen) through each individual line.

The moment the crack crosses a particular reference line, denotes the occurrence of a stress maximum, and corresponds to a specific fatigue cycle. In this way, the points on the line of crack crossing that particular reference line are determined, as well as the fatigue cycles for which the crack has crossed the specific reference line. Using these data, enabled estimation of the crack path as well as the crack growth rate.

From the maximum stress versus fatigue cycles curves for each reference line shown in Figure 7A, the crack lengths versus the number of fatigue cycles were determined for A359/SiCp composites heat

doi: 10.1111/j.1475-1305.2009.00665.x

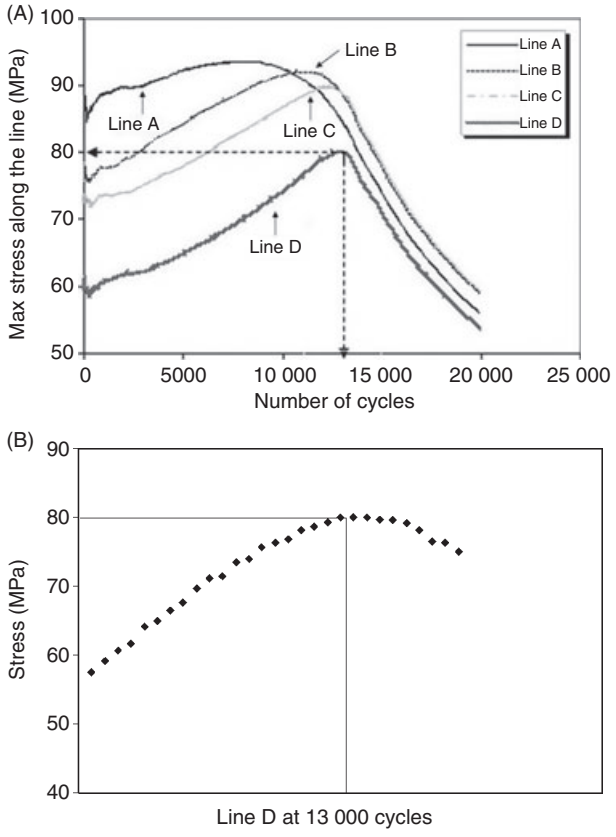

Figure 7: (A) Maximum Stress along the four reference lines versus fatigue N cycles. (B) Example of stress monitored along a reference line for a specific time, corresponding to a certain number of fatigue cycles

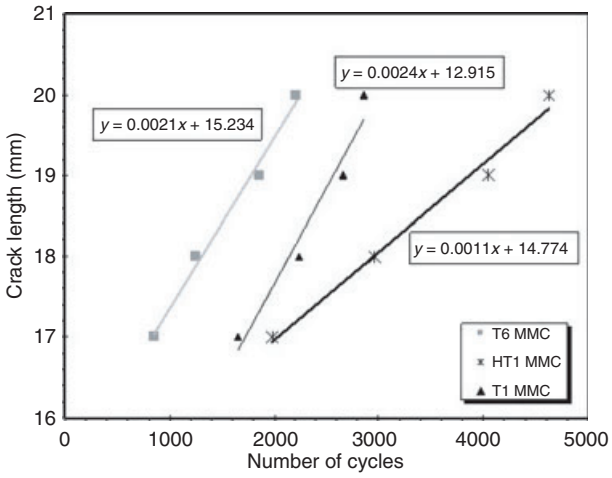

Figure 9: Crack length versus cycles plots from lock-in thermography data for A359/SiCp composites subjected to three different heat treatment conditions

treated in three different conditions; T1, T6, and HT-1 (Figure 9). As it is shown in Figure 9, the crack growth rate was found to be quite linear for all heat treatments. It is shown that the crack growth linear slope in both systems T1 and T6 is similar, but for the T6 condition the number of cycles required for the crack to be initiated is less than the T1 condition. On the other hand, there is a small change of the linear slope for the HT-1 heat treated sample, showing increased ductility which indicates that it needs more time (i.e. number of cycles) for the crack to grow in

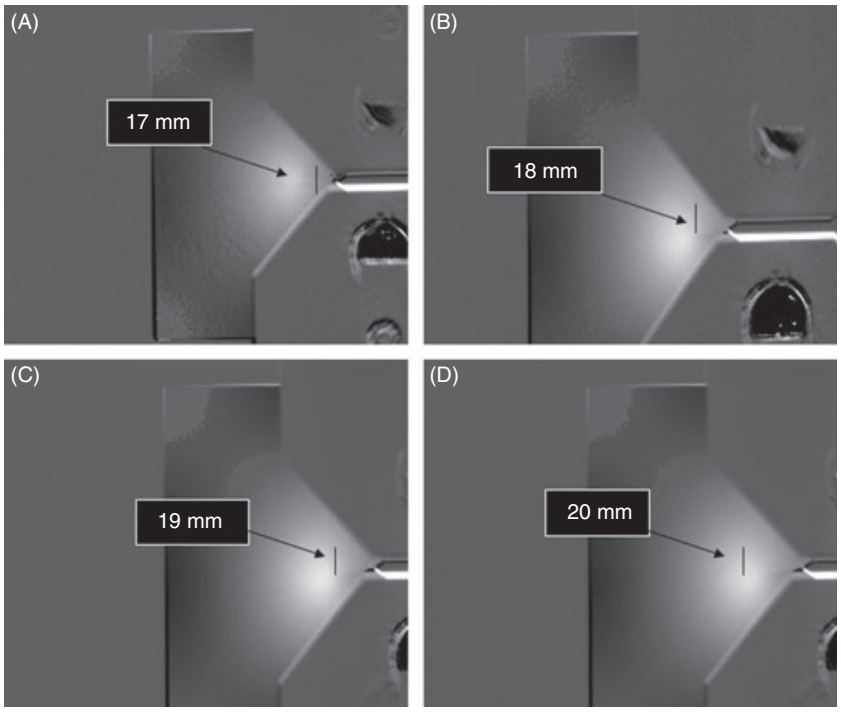

Figure 8: Thermographic images correspond to the four different reference lines showing the crack propagation length and the stress field for each of these lines

doi: 10.1111/j.1475-1305.2009.00665.x

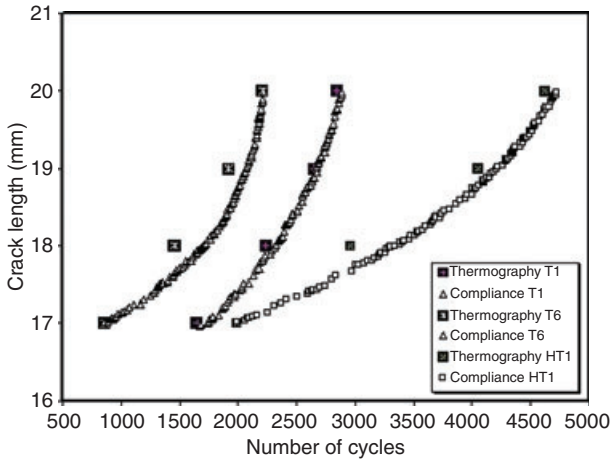

Figure 10: Crack growth rate determined by the compliance versus thermography methods for A359/SiC_P composite in as received (T1), T6 and HT1 heat treatments

this case. For the T6 heat treatment, the results depict a brittle behaviour, as the crack starts to grow earlier than in the other two cases, supporting evidence of brittle behaviour as it was also observed in previous work [22].

The data obtained using lock-in thermography, as shown in Figure 9, were correlated with crack growth rate values obtained by the conventional compliance method. Figure 10 show crack growth rates determined by the conventional compliance method versus the lock-in thermography method for A359/SiCp composites, as received, T6 heat treated, and HT-1 heat treated, respectively. Looking at these figures, one can observe that that there is a good correlation between the two methods for determining crack growth rate.

The actual difference between the values determined with the two methods is only of the order of about 50 cycles. Given the fact that the IR camera acquires a signal at a rate 20 times faster than the controller of the fatigue machine, it is expected that the thermographic measurement is more accurate in respect to the cycles, than the compliance measurement made by the fatigue machine. At the centre of the test this difference is more accentuated than at the beginning or the end of the experiment.

Conclusions

This study demonstrated that crack growth can be monitored by the means of lock-in thermography. The results obtained using the non-contact technique showed good match with the conventional compliance method. This new methodology can be dominant in situations when the compliance method cannot be used, e.g., crack growth in structures such as air wings and turbine engines during real-time applications, where non-destructive thermographic evaluation can be effective in monitoring crack propagation. In the field it is off course not feasible to use lock-in thermography since sinusoidal loading excitations do not exist. However, the main idea of lock-in process is to compare thermographic data in time, obtained at similar loading conditions. This process could be achieved in the field by correlating the loading history of a structure to the thermographic data obtained for the same time frame and comparing those thermographic data that correspond to similar loading conditions. The newly developed technique shows great potential in monitoring the crack growth rate of materials in regard to the crack depth, crack propagation time and path. The significant capability of this technique is the detection and monitoring of crack growth, even if it is not visible on the specimen's surface and propagates inside the material.

In our case the crack was propagating in a straight line. However, the technique is equally applicable regardless the cracks propagating in a straight line or not because it is based on detecting the presence of cracks due to modifications of the stress fields ahead of the crack tip and not of optical observation of the actual crack. This technique is capable of detecting surface as well as subsurface cracks in the material.

In this work it was also observed that heat treatment processing of metal matrix composites clearly affects their fracture properties. By appropriate heat treatment, the fracture behaviour of the material can be tailored and the fatigue crack growth rate can become either faster or slower (i.e. the material can become less or more ductile).

REFERENCES

1. Myriounis, D. P., Hasan, S. T. and Matikas, T. E. (2008) Microdeformation behaviour of Al–SiC metal matrix composites. *Compos Interfaces* **15**, 495–514.
2. Wong, B. S., Tui, C. G., Bai, W., Tan, P. H., Low, B. S. and Tan, K. S. (1999) Thermographic evaluation of defects in composite materials. *Insight: NDT-and Cond Monit.* **41**, 504–509.
3. Myriounis, D. P., Hasan, S. T. and Matikas, T. E. (2008) Heat treatment and interface effects on the mechanical behaviour of SiC particle reinforced aluminium matrix composites. *J. ASTM Int.* **5**, in print (published online 23 July 2008).
4. Taya, M. and Arsenault, R. J. (1989) *Metal Matrix Composites: Thermomechanical Behavior* vol. 4. Pergamon Press, Elmsford, New York.
5. Srivatsan, T. S. and Al-Hajri, M. (2002) The fatigue and final fracture behavior of SiC particle reinforced 7034 aluminum matrix composites. *Composites: Part B* **33**, 391–404.

doi: 10.1111/j.1475-1305.2009.00665.x

6. Christman, T. and Suresh, S. (1988) Effects of SiC reinforcement and aging treatment on fatigue crack growth in an Al—SiC composite. *Mater. Sci. Eng.* **102**, 211–220.
7. Srivatsan, T. S. (1992) The low-cycle fatigue behaviour of an aluminium-alloy-ceramic-particle composite. *Int. J. Fatig.* **14**, 173–182.
8. Zhang, R. J., Wang, Z. and Simpson, C. (1991) Fatigue fractography of particulate-SiC-reinforced Al (A356) cast alloy. *Mater. Sci. Eng A* **148**, 53–66.
9. Davidson, D. L. (1993) Fatigue and fracture toughness of aluminium alloys reinforced with SiC and alumina particles. *Composites* **24**, 248–255.
10. Manoharan, M. and Lewandowski, J. J. (1990) Fracture Initiation and Growth Toughness of an Aluminum Metal-Matrix Composite. *Acta Met.* **38**, 489–499.
11. Shang, J. K., Yu, W. and Ritchie, R. O. (1988) Role of silicon carbide particles in fatigue crack growth in SiC particulate reinforced aluminum alloy composite. *Mater. Sci. Eng.* **A102**, 181–192.
12. Stanley, P. and Chan, W. K. (1986) The determination of stress intensity factors and crack tip velocities from thermoelastic infra-red emissions, *Proc. Int. Conf. on Fatigue of Engineering Materials and Structures*, *IMechE*, Paper C262, 105–114.
13. Tomlinson, R. A. and Olden, E. J. (1999) Thermoelasticity for the analysis of crack tip stress fields – a review. *Strain*, **35**, 49–55.
14. Cavaliere, P., De Santis, A., Panella, F. and Squillace, A. (2009) Thermoelasticity and CCD analysis of crack propagation in AA6082 friction stir welded joints. *Int. J. Fatig.* **31**, 385–392.
15. Bremond, P. and Potet, P. (2001) Cedip Infrared Systems, Lock-in Thermography, A tool to analyze and locate thermo-mechanical mechanism in materials and structure Thermosence XXIII.
16. Myriounis, D. P., Hasan, S. T. and Matikas, T. E. (2007) *Role of Interfacial Properties on the Mechanical Behaviour of Al-Sic Metal-Matrix Composites*. *Proc. Int. Conf. Struct. Analy. Advanc. mat. (ICSAM-07*) Patras, Greece.
17. Merle, P. (2000) *MMC-Assess Thematic Network, Thermal Treatments of Age Hardenable Metal Matrix Composites*, Vol. 2. European Community, published online.
18. Maldague, X. V. (2001) *Theory and Practice of Infrared Technology for Nondestructive Testing*. John Wiley&Sons, Inc, New York.
19. Choi, M.-Y., Park, J.-H., Kang, K. S. and Kim, W.-T. (2006) Application of thermography to analysis of thermal stress in the NDT for compact tensile specimen. 12th A-PCNDT 2006 – Asia-Pacific Conference on NDT, 5th – 10th Nov, Auckland, New Zealand.
20. ASM Handbook (1989) *Nondestructive Evaluation and Quality Control*, Vol. 17. ASM International, Materials Park, OH, USA.
21. Annual Book of ASTM Standards ASTM E647 - 08 'Standard Test Method for Measurement of Fatigue Crack Growth Rates'.
22. Myriounis, D. P., Hasan, S. T. and Matikas, T. E. (2008) Influence of processing conditions on the micromechanical properties of particulate-reinforced aluminium matrix composites. *Adv. Compos. Lett.* **17**, 3.

doi: 10.1111/j.1475-1305.2009.00665.x